Chemical Science

Accepted Manuscript

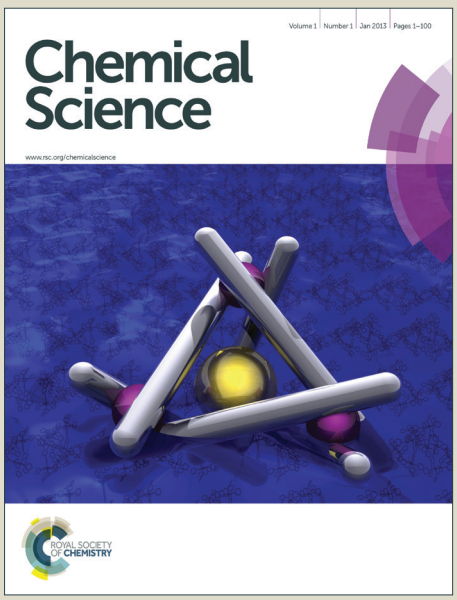

ROYAL SOCIETY OF CHEMISTRY

www.rsc.org/chemicalscience

Cite this: DOI: 10.1039/c0xx00000x

www.rsc.org/xxxxxx

EDGE ARTICLE

Hydrogen dangling bonds induce ferromagnetism in two-dimensional metal-free graphitic-C_3N_4 nanosheets

Kun Xu,[a] Xiuling Li,[b] Pengzuo Chen,[a] Dan Zhou,[a] Changzheng Wu,*[a] Yuqiao Guo,[a] Lidong Zhang,[c] Jiyin Zhao,[a] Xiaojun Wu,[ab] and Yi Xie[a]

Received (in XXX, XXX) Xth XXXXXXXXX 20XX, Accepted Xth XXXXXXXXX 20XX
DOI: 10.1039/b000000x

Ferromagnetic two-dimensional (2D) ultrathin nanosheets hold great promise for next generation electronics. Ferromagnetic metal-free materials that usually possess only s/p electronic configuration with weak spin-orbit coupling and large spin relaxation time, which would play an important role in constructing future spintronics devices. However, the absence of intrinsic spin ordering structure in most metal-free materials greatly hampers widening the scope of ferromagnetic 2D nanostructures as well as in-depth understanding of ferromagnetic nature. Herein, inducing intrinsic ferromagnetism in 2D metal-free g-C_3N_4 ultrathin nanosheets has been achieved through a new effective strategy of introduction of hydrogen dangling bonds. In our case, g-C_3N_4 ultrathin nanosheets with hydrogen dangling bonds show obvious room temperature ferromagnetic behavior that can even be tuned by the hydrogen concentrations. This work will pave a new pathway to engineer the properties of the 2D nanomaterials systems.

Introduction

Two dimensional (2D) ultrathin nanosheets are of great interest in bringing about exotic physical properties arising from their dimensional reduction systems, which hold enormous promise for next generation electronic devices.[1-3] Recent investigations of ferromagnetic 2D nanomaterials with unique spin ordering have received extensive attention owing to their potential application in future spintronic devices.[4,5] However, although significant efforts have been made to develop 2D ferromagnetic nanosheets with 3d electronic configuration,[6-8] ferromagnetic 2D metal-free ultrathin nanosheets only with s/p electronic structure present relatively weak spin-orbit coupling and could give large spin relaxation time that are more suitable for future-generation spintronic devices.[9] Unfortunately, metal-free materials usually lack ordered spin structure in their pristine forms, greatly hampering appearance of ferromagnetic behavior in their 2D nanostructure. Thus, it is highly desirable to achieve magnetic coupling modulation in 2D metal-free ultrathin nanosheets for future-generation spintronic devices.

Hydrogenation provides a new intriguing strategy to regulate electronic structure of materials, endowing new opportunity to induce spin related information in 2D metal-free ultrathin nanosheets.[10,11] Serial theoretical calculations have already predicated that hydrogenation of graphene could induce ferromagnetic behavior.[12,13] In this case, hydrogenation of graphene, i.e. modifying hydrogen atoms onto in-plane surface carbon atoms, would be extremely experimental challenging because that configuration changes from sp^2 to sp^3 hybridization requires to overcome a considerable energy barrier.[14] However, graphite carbon nitride (g-C_3N_4), a graphite-like material with C-N layers weakly stacked structure, shows advancements for hydrogenation.[15,16] For g-C_3N_4, there is only one non-bonding electron in C atom with sp^2 hybridized structure while lone pair electrons or more electrons would be remnant in N atom with sp^3 or sp^2 hybridized structure. In this regard, manipulating hydrogen dangling bonds interaction in g-C_3N_4 ultrathin nanosheets is much easier than that in graphene from experimental viewpoint. In effect, g-C_3N_4 has attracted tremendous attention due to its unique electronic band structure catering for intriguing applications in catalysis, sensor, bioimaging and so on.[17-20] Thus,

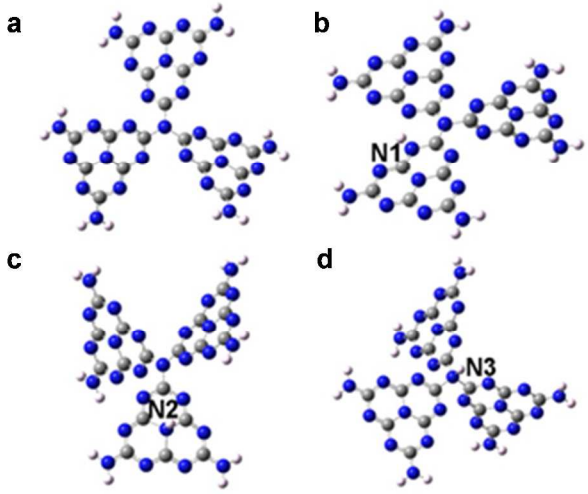

Figure 1. The calculated molecular model of (a) g-C_3N_4, (b) g-C_3N_4 with hydrogen dangling bonds in N1 site, (c) hydrogen dangling bonds in N2 site, and (d) hydrogen dangling bonds in N3 site. Gray, blue and white balls represent C, N and H atoms, respectively.

it remains an open question whether hydrogen dangling bonds could endow spin-related information in graphene-like g-C_3N_4 structure.

Density-functional theory based on the g-C_3N_4 structure model consisting of 3 tris-s-triazine (melem) unites revealed that hydrogen dangling bonds in N2 sites would not bring spin-related information. Interestingly, the hydrogen bonds in N1 and N3 sites could induce ferromagnetism. Further theoretical calculations were carried out with the M062X/6-31G(d,p) method in the Gaussian 09 program package to study total energy of the hydrogen dangling bonds in different N sites of g-C_3N_4 structure (Figure 1).[21-22] The hydrogen bonds in N1 sites are more stable than those in N2 and N3 sites, with energy differences of 43.06 kcal/mol and 38.96 kcal/mol, respectively. Based on above analysis, engineering of hydrogen dangling bonds in g-C_3N_4 ultrathin nanosheets shows a promising sign to induce intrinsic ferromagnetism in 2D metal-free nanomaterials. Herein, a new room temperature ferromagnetic 2D nanomaterial, g-C_3N_4 ultrathin nanosheets with hydrogen dangling bonds, was confirmed for the first time. In our case, the spin ordering structure was endowed in 2D g-C_3N_4 ultrathin nanosheets by introducing the hydrogen dangling bonds. Interestingly, the saturation magnetization of g-C_3N_4 could even be tuned by increasing the hydrogen dangling bonds content. The hydrogen dangling bonds in g-C_3N_4 ultrathin nanosheets brought an impressive saturation magnetization value of 0.015 emu/g associated with a coercivity of 87 Oe at room temperature. To the best of our knowledge, it is the first experimental case to corroborate that hydrogen dangling bonds could achieve magnetic coupling modulated in 2D metal-free g-C_3N_4 systems.

Results and discussion

G-C_3N_4 ultrathin nanosheets with hydrogen dangling bonds (denoted as CN-3) are obtained by the liquid exfoliation of bulk g-C_3N_4 (denoted as CN-1). The g-C_3N_4 ultrathin nanosheets with more hydrogen dangling bonds (denoted as CN-4) are obtained by the liquid exfoliation of protonated bulk g-C_3N_4 (denoted as CN-2). The hydrogen content of the CN-4 is higher than that of CN-3, which was confirmed by elemental analysis (Table S1). Subsequently, systematical characterizations were performed to verify that CN-4 was in ultrathin nanosheet structure and the C-N framework was still maintained. The colloidal suspension solution of CN-4 (Figure 2a inset) could remain stable, without aggregation for several weeks, providing solid evidence for homogeneously exfoliated 2D nanosheets. Transmission electron microscope (TEM) image of CN-4 shown in Figure 2a revealed that the lateral diameters of CN-4 are ~ 200 nm. Atomic force microscopy (AFM) also confirmed that the nanosheet diameter is ~ 200 nm, which was consistent with the results from TEM analyses. Meanwhile, the thickness of the products was measured by the AFM. As can be seen from Figure 2b and 2c, the thicknesses of ultrathin nanosheets are ranging from 2.2 nm to 3.0 nm, which indicates the ultrathin nanosheets are composed of 6~9 CN atomic monolayers.

Structural information of CN-4 was elucidated by X-ray diffraction (XRD) and Raman spectroscopy. As shown in Figure 2d, XRD pattern of CN-4 only presented (002) peak, suggesting high orientation and ultrathin morphology of as-exfoliated g-C_3N_4. In the Raman spectrum of CN-4, the peaks located at 705 cm^{-1}, 755 cm^{-1}, 1233 cm^{-1} and 1350 cm^{-1} match well with those in previous literature for g-C_3N_4, suggesting CN-4 was still composed of basic C-N atomic layers (Figure 2e).[19, 23] Also, electron energy loss spectra (EELS) confirmed that only carbon and nitrogen elements existed in CN-4 (Figure 2f). All above results verified that the g-C_3N_4 ultrathin nanosheets with more

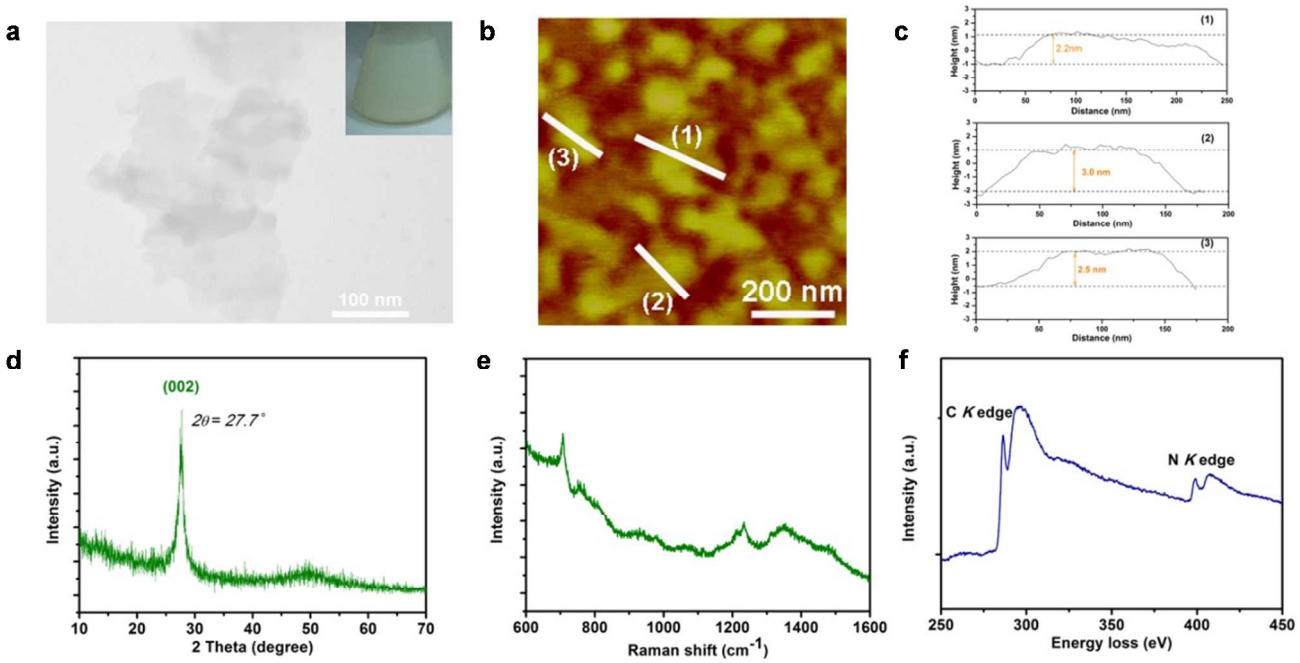

Figure 2. Characterization of CN-4. (a) TEM image. Inset: homogeneously dispersed CN-4 nanosheets suspension. (b) and (c) AFM image and the corresponding height profile. (d) XRD pattern. (e) Raman spectra. (f) EELS spectra.

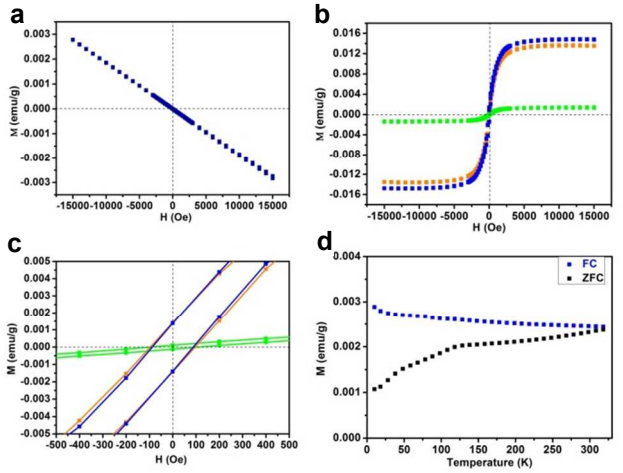

Figure 3. (a) M-H curves of CN-1 at 300 K. (b) M-H curves of CN-2, CN-3 and CN-4 at 300 K. Green, orange and blue curves represent CN-2, CN-3 and CN-4, respectively. (c) Enlarge central section of (b). (d) Temperature dependence of zero field cooling (ZFC) and field cooling (FC) curves of CN-4 under the measuring field of 200 Oe. Note: M means magnetization and H means applied magnetic field.

hydrogen dangling bonds (CN-4) were successfully prepared with high quality.

It is well known that substantial amino ($-NH_2$) group usually existed at edge sites of bulk g-C_3N_4, which is derived from thermal polycondensation of dicyandiamide.[23, 24] In consideration of the total energy of the hydrogen dangling bonds in different N sites of g-C_3N_4 structure, the formation of hydrogen dangling bonds in N1 sites is also attainable due to the easy promotion of more protons combining with N atoms under high power ultrasonication in aqueous solution during the exfoliation process. In order to test our expectation that hydrogen dangling bonds would bring ferromagnetic properties in g-C_3N_4 ultrathin nanosheets, superconducting quantum interference device (SQUID) was used to investigate the magnetic properties of the CN-2, CN-3, CN-4 as well as the CN-1. Figure 3a shows magnetic field dependence of magnetization (M-H) curve of CN-1 at 300K, clearly demonstrating that the virgin bulk g-C_3N_4 is diamagnetic which implies the purity of bulk sample. As shown in Figure 3b and 3c, the expected ferromagnetic behaviors of the CN-2, CN-3 and CN-4 are fully confirmed by corresponding M-H curves, where all M-H curves exhibit saturation magnetization and clear hysteresis loop. The saturation magnetization (Ms) value of CN-4 at room temperature was as high as 0.015 emu/g with coercivity of 87 Oe. Very weak ferromagnetism in CN-2 was understandable by the fact that only simple agitation could not provide sufficient energy to form many hydrogen dangling bonds in N1 sites of bulk g-C_3N_4. In addition, temperature dependent magnetization (M-T) curves of the CN-4 presented in Figure 3d provide another evidence to prove the sample is intrinsically room-temperature ferromagnetism. Obviously, zero field cooling (ZFC) and field cooling (FC) curves showed distinct difference in wide temperature range from 10 up to 330 K, revealing Curie temperature is higher than 330K. Most importantly, there is no block temperature appearance in ZFC curve, which clearly reveals that there are no ferromagnetic

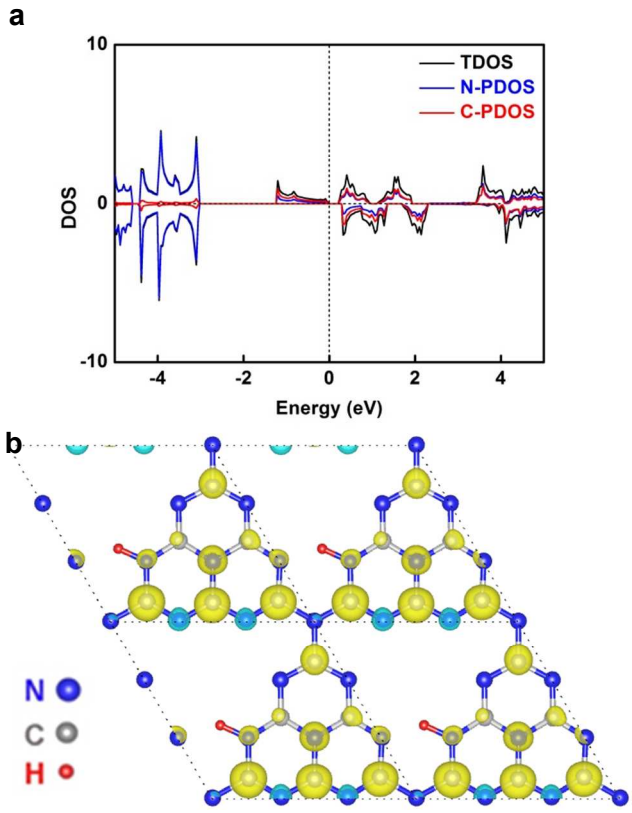

Figure 4. (a) TDOS and PDOS of g-C_3N_4 single layer with hydrogen dangling bonds in N1 site. The Fermi level is set at 0 eV. (b) The corresponding spin density distribution. Note: TDOS represents total density of states and PDOS represents the corresponding atomic projected density.

clusters in our sample and provides evidence for ferromagnetism in the CN-4.[25] Of note, the ferromagnetic impurities such as Fe, Co, Ni could also be excluded by inductively coupled plasma (ICP) results (Table S2). Therefore, all above analyses confirmed that the room temperature ferromagnetism in CN-4 is inherent nature.

In our case, hydrogen dangling bonds in four samples from CN-1 to CN-4 with gradual increasing hydrogen concentrations indeed regulated the ferromagnetic behaviour. To further understand how hydrogen dangling bonds influence the ferromagnetism in CN-2, CN-3 and CN-4, single layer g-C_3N_4 with hydrogen dangling bonds in N1 site was used as the calculation model to study the origin of ferromagnetism in carbon nitrides. As shown in Figure 4a, a significant asymmetry between the spin-up state and spin-down state in the density of states (DOS) near the Fermi level suggests the intrinsic ferromagnetism of g-C_3N_4 single layer with hydrogen dangling in N1 site. As well known, the value of the Curie temperature depends on the exchange stiffness and the DOS at the Fermi level. The calculated DOS display obvious spin splitting at the conduction band and valence band means the relative high Curie temperature in this configuration, which is identical with our experimental results. The total magnetic moments of this electronic structure are about 1.0 uB. The spin-resolved DOS projected on the p orbitals of C and N is also presented in the Figure 4a. Both of the N-PDOS and C-PDOS

shows significant asymmetry between the spin-up state and spin-down state near the Fermi level, illustrating both of them contribute the magnetic moment to the total magnetic moment. Obviously, the magnetic moment in the structure is mostly attributed to the p orbital of C atoms and the maximal magnetic moment of C atom is about 0.15 uB. Furthermore, the spin density distribution (Figure 4b) also indicates the main magnetism is originated from the C atoms in this structure, which is identical with the DOS. Thus, involving of hydrogen dangling bonds induce intrinsic ferromagnetism in g-C_3N_4 ultrathin nanosheets, which is verified by both magnetic characterizations and theoretical calculations.

Controlling concentration of hydrogen dangling bonds regulated intrinsic ferromagnetism in 2D carbon nitrides, with exclusion of all alternative possibility that would arise spin ordering. Of note, three influence factors including heteroatom incorporation, non-metal elemental adsorption and defect are well known approaches to induce magnetism in raw non-magnetic materials. For our carbon nitrides, these three factors were not responsible for intrinsic ferromagnetism, which was based on the detailed explanation in the followings: Firstly, the EELS spectra of CN-3 and CN-4 (Figure 2f and S9) provided solid evidence that no heteroatoms were introduced during sample preparation process. And therefore the ferromagnetic behavior in our sample was not triggered by heteroatom incorporation or non-metal elemental adsorption. Secondly, the molar ratios of N/C of CN-1, CN-2, CN-3 and CN-4 are all approximately 1.52, given by elemental analysis. If N rich (C defect) indeed induced ferromagnetism, CN-1 would behave intrinsic ferromagnetic behaviour. However, as a fact, CN-1 showed intrinsic diamagnetism with contrary experimental results (Figure 3a). And thus, these analyses gave evidences to exclude the possibility that the ferromagnetism of CN-2, CN-3 and CN-4 was derived from defects. With exclusion of influence factors mentioned above, the gradually increasing content of hydrogen dangling bonds in our as-obtained g-C_3N_4 from CN-2 to CN-4 was capable of enhancing ferromagnetism, which revealed that hydrogen dangling bonds was able to trigger spin regulation. Indeed, magnetic coupling modulation in metal-free ultrathin nanosheets would be a significant step for future electronics and spintronics.

Conclusions

In summary, we have demonstrated that the introduction of hydrogen dangling bonds could become a new strategy to regulate magnetic properties in 2D metal-free systems. And g-C_3N_4 ultrathin nanosheets with hydrogen dangling bonds, as a new metal-free room temperature ferromagnetic 2D nanomaterial, have also been confirmed for the first time. The saturation magnetization value of g-C_3N_4 ultrathin nanosheets at room temperature was as high as 0.015 emu/g. The 2D metal-free g-C_3N_4 ultrathin nanosheets with intrinsic room temperature ferromagnetism which could carry spin-related information are highly desirable as a building block for constructing next generation electronic and spintronic devices. This work will broaden our horizon to achieve magnetic couple modulation in metal-free materials. Meanwhile, we anticipate that the introduction of hydrogen dangling bonds strategy could be an effective way for engineering the intrinsic physicochemical properties in 2D nanomaterials.

Acknowledgements

This work was financially supported by the National Natural Science Foundation of China (no. 21222101, 11132009, 21331005, 11321503, J1030412), Chinese Academy of Science (XDB01010300), the Fok Ying-Tong Education Foundation, China (Grant No.141042) and the Fundamental Research Funds for the Central Universities (no. WK2060190027 and WK2310000024).

Notes and references

[a] *Hefei National Laboratory for Physical Sciences at Microscale, University of Science and Technology of China, Hefei, P. R. China. E-mail: czwu@ustc.edu.cn*

[b] *CAS Key Laboratory of Materials for Energy Conversion and Depart of Material Science and Engineering, University of Science and Technology of China, Hefei, P. R. China.*

[c] *National Synchrotron Radiation Laboratory, University of Science and Technology of China, Hefei, P. R. China.*

† Electronic Supplementary Information (ESI) available: Experimental and characterization. See DOI: 10.1039/b000000x/

1 M. Chhowalla, H. S. Shin, G. Eda, L.-J. Li, K. P. Loh, and H. Zhang, Nat. Chem., 2013, 5, 263-275.
2 X. Zhang and Y. Xie, Chem. Soc. Rev., 2013, **42**, 8187-8199.
3 H. Li, J. Wu, Z. Yin, and H. Zhang, *Acc. Chem. Res.*, 2014, **47**, 1067-1075.
4 Q. H. Wang, K. Kalantar-Zadeh, A. Kis, J. N. Coleman, and M. S. Strano, *Nat. Nanotechnol.*, 2012, **7**, 699-712.
5 Y. Ma, Y. Dai, M. Guo, C. Niu, Y. Zhu, and B. Huang, *ACS Nano*, 2012, **6**, 1695-1701.
6 K. Xu, P. Chen, X. Li, C. Wu, Y. Guo, J. Zhao, X. Wu, and Y. Xie, *Angew. Chem. Int. Ed.*, 2013, **52**, 10477-10481.
7 X. Zhang, J. Zhang, J. Zhao, B. Pan, M. Kong, J. Chen, and Y. Xie, *J. Am. Chem. Soc.*, 2012, **134**, 11908-11911.
8 P. Chen, K. Xu, X. Li, Y. Guo, D. Zhou, J. Zhao, X. Wu, C. Wu and Y. Xie, Chem. Sci., 2014, **5**, 2251-2255.
9 A. Du, S. Sanvito, and S. C. Smith, *Phys. Rev. Lett.*, 2012, **108**, 197207.
10 J. Wei, H. Ji, W. Guo, A. H. Nevidomskyy, and D. Natelson, *Nat. Nanotechnol.*, 2012, **7**, 357-362.
11 C. Lin, X. Zhu, J. Feng, C. Wu, S. Hu, J. Peng, Y. Guo, L. Peng, J. Zhao, J. Huang, J. Yang, and Y. Xie, *J. Am. Chem. Soc.*, 2013, **135**, 5144-5151.
12 J. Zhou, Q. Wang, Q. Sun, X. S. Chen, Y. Kawazoe, and P. Jena, *Nano Lett.*, 2009, **9**, 3867-3870.
13 M. Gmitra, D. Kochan, and J. Fabian, *Phys. Rev. Lett.*, 2013, **110**, 246602.
14 M. Wojtaszek, I. J. Vera-Marun, T. Maassen, and B. J. van Wees, *Phys. Rev. B*, 2013, **87**, 081402.
15 X. Wang, K. Maeda, A. Thomas, K. Takanabe, G. Xin, J. M. Carlsson, K. Domen, and M. Antonietti, *Nat. Mater.*, 2009, **8**, 76-80.
16 M. Groenewolt, and M. Antonietti, *Adv. Mater.*, 2005, **17**, 1789-1792.
17 X.-H. Li, X. Wang and M. Antonietti, Chem. Sci., 2012, **3**, 2170-2174.
18 J. Zhang, M. Grzelczak, Y. Hou, K. Maeda, K. Domen, X. Fu, M. Antonietti and X. Wang, Chem. Sci., 2012, **3**, 443-446.
19 X. Zhang, X. Xie, H. Wang, J. Zhang, B. Pan, and Y. Xie, *J. Am. Chem. Soc.* 2012, **135**, 18-21.
20 X. Zhang, H. Wang, H. Wang, Q. Zhang, J. Xie, Y. Tian, J. Wang, and Y. Xie, Adv. Mater., 2014, **26**, 4438-4443.
21 Y. Zhao, and D. Truhlar, *Theor. Chem Acc.*, 2008, **120**, 215-241.
22 Frisch, M. J.; Trucks, G. W.; Schlegel, H. B.; Scuseria, G. E.;Robb, M. A.; Cheeseman, J. R.; Scalmani, G.; Barone, V.; Mennucci, B.; Petersson, G. A.; Nakatsuji, H.; Caricato, M.; Li, X.; Hratchian, H. P.; Izmaylov, A. F.; Bloino, J.; Zheng, G.; Sonnenberg, J. L.; Hada,

M.; Ehara, M.; Toyota, K.; Fukuda, R.; Hasegawa, J.; Ishida, M.;Nakajima, T.; Honda, Y.; Kitao, O.; Nakai, H.; Vreven, T.; Montgomery, J. A., Jr.; Peralta, J. E.; Ogliaro, F.; Bearpark, M.; Heyd, J. J.; Brothers, E.; Kudin,K. N.; Staroverov, V. N.; Keith, T.; Kobayashi, R.; Normand, J.; Raghavachari, K.; Rendell, A.; Burant, J. C.; Iyengar, S. S.; Tomasi, J.; Cossi, M.; Rega, N.; N.; Millam, J. M.; Klene, M.; Knox, J. E.; Cross, J. B.; Bakken, V.; Adamo, C.; Jaramillo, J.; Gomperts, R.; Stratmann, R. E.; Yazyev, O.; Austin, A. J.; Cammi, R.; Pomelli, C.; Ochterski, J. W.; Martin, R. L.; Morokuma, K.; Zakrzewski, V. G.; Voth, G. A.; Salvador, P.; Dannenberg, J. J.; Dapprich, S.; Daniels, A. D.; Farkas, O.;Foresman, J. B.; Ortiz, J. V.; Cioslowski, J.; and Fox, D. J. Gaussian09, Revision B.01, Gaussian, Inc.: Wallingford, CT, 2010.

23 T. Y. Ma, Y. Tang, S. Dai, and S. Z. Qiao, *Small*, 2014, **10**, 2382-2389.

24 Y. Shi, S. Jiang, K. Zhou, C. Bao, B. Yu, X. Qian, B. Wang, N. Hong, P. Wen, Z. Gui, Y. Hu, and R. K. K. Yuen, *ACS Appl. Mater. Interfaces*, 2013, **6**, 429-437.

25 T. Taniguchi, K. Yamaguchi, A. Shigeta, Y. Matsuda, S. Hayami, T. Shimizu, T. Matsui, T. Yamazaki, A. Funatstu, Y. Makinose, N. Matsushita, M. Koinuma, and Y. Matsumoto, *Adv. Funct. Mater.*, 2013, **23**, 3140-3145.